

made with the rf wave traveling in the same direction as the beam. For the data shown in the figure, the solid curve represents a computer least-squares fit of the experimental points by a Lorentzian curve of variable amplitude, width, baseline, and position. The results given in Tables I and II were, however, obtained from a graphical analysis of the resonance curves.

The errors quoted are larger than the statistical errors in finding the peak centers; they arise from errors in rf power leveling (especially serious for $n=4$), uncertainties in profile shapes, corrections due to motional Stark effect from an uncanceled Earth's field, and with the exception of results for 6560 Å, errors in the Doppler shifts arising from small uncertainties in beam velocity. For 6560 Å, however, this source of error was avoided by taking measurements for both directions of rf wave.

We have shown that the method of Fabjan and Pipkin may be readily extended to measurements of fine structures in electronically excited states of ${}^4\text{He}^+$, and presented the first rf measurements of such structures in $n=6$ and 7. Although the precision of the results we have so far obtained is not high enough to constitute a test of quantum electrodynamic calculations for the Lamb shifts measured, there seems no fundamental reason why the measurements of Jacobs, Lea, and Lamb³ for $n=4$ and of Baumann and Eibofner⁴ for $n=5$ cannot be improved upon by the present technique; the possibility of using double quantum transitions, as suggested recently by Kramer *et al.*⁶ could even eventually lead to an improved value

TABLE II. Fine structures for $n=6$ of ${}^4\text{He}^+$ measured in the 6560-Å transition.

Transition	Measured frequency (MHz)	Theory ^a (MHz)
$g_{9/2}-h_{11/2}$	437 ± 10	432.3
$f_{7/2}-g_{9/2}$	648.5 ± 5	648.5
$g_{7/2}-h_{9/2}$		649.0

^aRef. 5.

for the fine-structure constant. Nonetheless, for the higher values of n studied, the presence of many closely spaced components makes precise measurements of the fine-structure separations rather difficult.

¹For an up-to-date survey, see V. W. Hughes, in *Proceedings of the Third International Conference on Atomic Physics, Colorado, 1972*, edited by S. J. Smith (Plenum, New York, 1973); N. M. Kroll, *ibid.*

²C. W. Fabjan and F. M. Pipkin, *Phys. Rev. A* **6**, 556 (1972).

³R. Jacobs, K. Lea, and W. Lamb, Jr., *Phys. Rev. A* **3**, 884 (1971).

⁴M. Baumann and A. Eibofner, *Phys. Lett.* **43A**, 105 (1973).

⁵The values given in the tabulation of J. Garcia and J. Mack, *J. Opt. Soc. Amer.* **55**, 654 (1965), are sufficiently accurate for our purposes.

⁶P. Kramer, S. Lundeen, B. Clark, and F. Pipkin, *Phys. Rev. Lett.* **32**, 635 (1974).

Elastic and Inelastic Electron Scattering at 20 and 60 eV from Atomic Cu†

W. Williams and S. Trajmar

Jet Propulsion Laboratory, California Institute of Technology, Pasadena, California 91103

(Received 2 May 1974)

Normalized differential and integral electron-impact cross sections for elastic scattering and for the excitation of the ${}^2D_{5/2}$, ${}^2D_{3/2}$, and ${}^2P_{3/2,1/2}$ levels of atomic copper have been determined at 20 and 60 eV. An unexpectedly large cross section was found for the excitation of the ${}^2P_{3/2,1/2}$ levels, which at certain angular and energy ranges surpasses the cross section for elastic scattering. The integral cross sections in units of 10^{-16} cm² are elastic, 91.0 and 59.0; ${}^2D_{5/2}$, 1.85 and 0.36; ${}^2D_{3/2}$, 1.26 and 0.26; ${}^2P_{3/2,1/2}$, 77.2 and 36.5, at 20 and 60 eV, respectively.

Besides a general interest in Cu in atomic physics, a need for electron-impact scattering cross sections has developed recently in connection

with Cu vapor lasers.¹⁻⁵ We are not aware of any experimental measurements on electron scattering by atomic Cu. Here, we present normal-

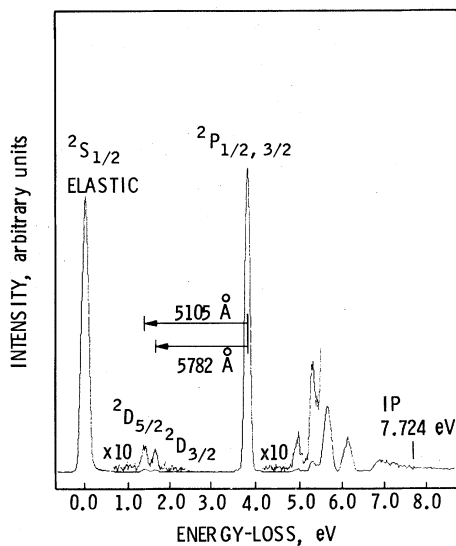


FIG. 1. Energy-loss spectrum of Cu at 20 eV impact energy and 18° scattering angle.

ized differential and integral cross sections at 20- and 60-eV impact energies for elastic scattering and for the excitation of the 2P and 2D states (upper and lower laser levels, respectively, for the 5106-Å and 5782-Å lasers).

The angular distribution for elastic scattering shows oscillations similar to those observed for other heavy elements. It has been found that at certain energy and angular ranges the cross section for the unresolved ${}^2P_{3/2}$ and ${}^2P_{1/2}$ excitations is larger than that for elastic scattering (see Figs. 1-3). An inelastic cross section of this magnitude, particularly when considered relative to the elastic cross section, is quite unexpected and may be an important factor from the point of view of laser applications. The cross sections for the ${}^2D_{5/2}$ and ${}^2D_{3/2}$ excitations are very similar. They are both strongly forward peaked and about an order of magnitude smaller than those for the combined 2P excitation. Previous estimations of the 2P and 2D excitations based on semiclassical¹ calculations differ significantly from these results.

The measurements were carried out in a crossed-beam configuration and with utilization of an electron-impact spectrometer similar to the one described earlier.⁶ An atomic Cu beam was generated by the heating of a tantalum crucible containing Cu by electron bombardment to approximately 1250°C. The Cu vapor diffused through a 0.1-cm diam, 0.5-cm-long channel to form the target beam. An energy-selected elec-

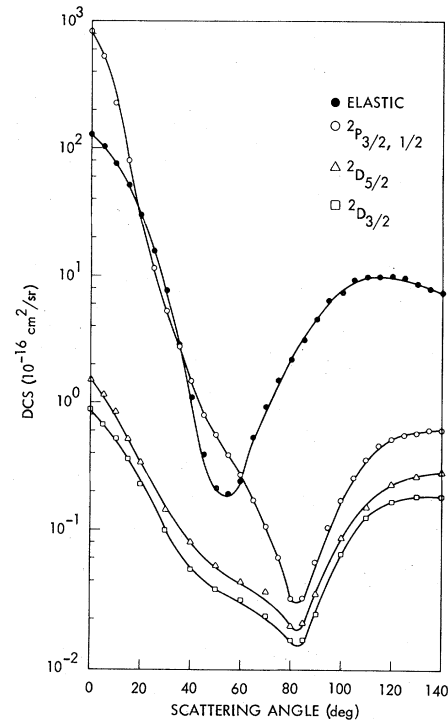


FIG. 2. Differential cross sections for elastic scattering, and for the excitation of the (${}^2P_{3/2} + {}^2P_{1/2}$), ${}^2D_{5/2}$, and ${}^2D_{3/2}$ states at 20 eV. The elastic scattering points below 10° are obtained by extrapolation.

tron beam (full width at half-maximum around 80 meV) crossed the Cu beam at right angles at about 0.2 cm above the tip of the crucible. The electron beam was monitored and trapped by a Faraday cup.

The scattering intensities at fixed impact energy (E_0) and scattering angle (θ) were determined as a function of energy loss (ΔE) by the use of pulse counting by multichannel-scaling techniques. Energy-loss spectra were obtained by our superimposing several energy-loss scans with the aid of the 1024-channel scaler. The impact-energy scale is believed to be accurate to ± 0.5 eV. The angular resolution can be estimated as described earlier⁷ to be between 1.7 to 3.2°. A typical spectrum is shown in Fig. 1. The two components of the 2P transition are separated only by 0.031 eV and are not resolved in the present measurements. Double-scattering features similar to the one observed by Hertel and Ross for potassium⁸ (${}^2P + {}^2P$) were not observed and therefore their effects can be neglected compared with other errors involved in the measurements.

Ratios of the inelastic-scattering intensities to the elastic-scattering intensity were determined

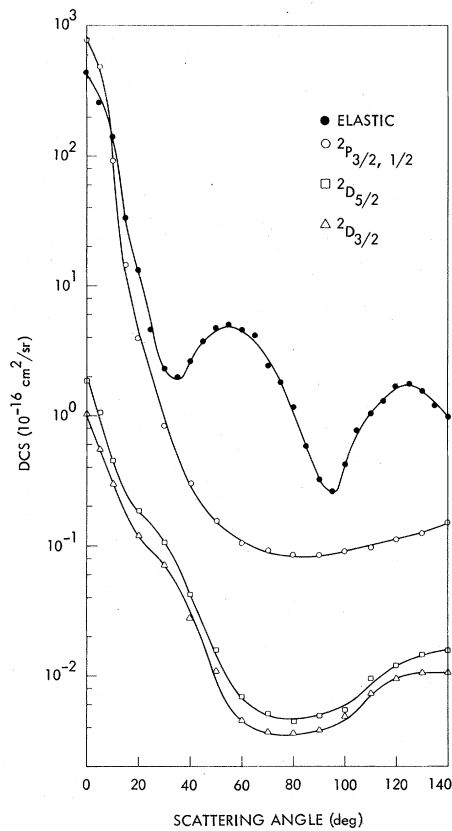


FIG. 3. Differential cross sections for elastic scattering, and for the excitation of the (${}^2P_{3/2} + {}^2P_{1/2}$), ${}^2D_{5/2}$, and ${}^2D_{3/2}$ states at 60 eV. The elastic scattering points below 10° are obtained by extrapolation.

for each spectrum in the range 10 to 140° . The elastic-scattering angular dependence in the same angular range was measured in a time short compared to the instrumental drift. The measurements were repeated several times until a reliable elastic-scattering distribution was obtained. Data below 10° were not taken because of direct-beam contribution. The elastic-scattering intensities were converted to differential cross sections in arbitrary units with an effective scatter-

ing-path-length correction. The accurate determination or calibration of the effective path-length correction is not feasible in the present apparatus, but one determined in another apparatus with similar scattering geometry was used. The low-angle behavior of the inelastic cross sections were determined down to 0° (no direct-beam contribution). The actual 0° scattering angle was determined by finding the point of symmetry in the 2P angular scattering distribution around 0° .

The elastic differential cross sections were extrapolated to 0° and to 180° and integrated to obtain integral cross sections. These integral elastic cross sections were normalized to the integral elastic cross-section values calculated by Winter and Cartwright.⁹ The intensity ratios combined with the normalized elastic cross sections yielded normalized inelastic cross sections. The details of this calculation and the justification for the normalization procedure will be discussed elsewhere.⁹ Based on comparison of integral elastic cross sections obtained by this calculational method to experimental data, in case of potassium, we believe that the absolute value of the normalized cross sections is accurate to within ± 50 and $\pm 75\%$ for 60 and 20 eV, respectively. When more accurate calculations or experimental procedures become available, the cross sections can be easily renormalized. The relative values of the cross sections are estimated to be accurate to within $\pm 20\%$ on the basis of a procedure described previously.⁷ A normalization to the optical f value was employed by Hertel and Ross⁸ for potassium. We found that this procedure for the 2P excitation was not more reliable than the one which we followed above even though our measurements extend to lower momentum-transfer values than those of Hertel and Ross. The normalized 2P cross section when plotted as a function of momentum transfer can, however, be extrapolated reasonably well to the optical f value of 0.711 as given by Corliss.¹⁰

TABLE I. Summary of integral cross sections (in units of 10^{-16} cm^2).

E_0 (eV)	Present Results						Leonard	
	Elastic	Momentum transfer	${}^2P_{3/2,1/2}$	${}^2D_{5/2}$	${}^2D_{3/2}$	${}^2D_{5/2}$	${}^2P_{3/2}$	
20	91.0	84.7	77.2	1.85	1.26	0.2	6.2	
60	59.0	17.5	36.5	0.36	0.26	0.014	4.0	

Figures 2 and 3 show the results for 20- and 60-eV impact energies, respectively.

The integral cross sections are summarized in Table I. A more detailed description of the results as well as cross sections at other impact energies and for other electronic transitions will be published later.

†This paper presents the results of one phase of research carried out at the Jet Propulsion Laboratory, California Institute of Technology, under Contract No. NAS7-100, sponsored by the National Aeronautics and Space Administration.

¹D. A. Leonard, IEEE J. Quantum Electron. **3**, 380 (1967).

²W. T. Walter, IEEE J. Quantum Electron. **4**, 355

(1968).

³A. A. Isaev, M. A. Kazaryan, and G. G. Petrash, Pis'ma Zh. Eksp. Teor. Fiz. **16**, 40 (1972) [JETP Lett. **16**, 27 (1972)].

⁴G. G. Petrash, Usp. Fiz. Nauk **105**, 645 (1971) [Sov. Phys. Usp. **14**, 747 (1972)].

⁵C. J. Chen, N. M. Nerheim, and G. Russel, Appl. Phys. Lett. **23**, 514 (1973).

⁶A. Chutjian, D. C. Cartwright, and S. Trajmar, Phys. Rev. Lett. **30**, 195 (1973).

⁷S. Trajmar, Phys. Rev. A **8**, 191 (1973).

⁸I. V. Hertel and K. J. Ross, J. Phys. B: Proc. Phys. Soc., London **2**, 285 (1969).

⁹N. Winter and D. C. Cartwright, private communication, and to be published. We are grateful to Dr. Winter and Dr. Cartwright for supplying us with their results prior to publication.

¹⁰C. H. Corliss, J. Res. Nat. Bur. Stand., Sect. A **74**, 781 (1970).

Observation of Stimulated Anti-Stokes Raman Scattering in Inverted Atomic Iodine*

R. L. Carman† and W. H. Lowdermilk

Lawrence Livermore Laboratory, University of California, Livermore, California 94550

(Received 23 May 1974)

Nonresonant stimulated anti-Stokes Raman scattering from an inverted population in atomic iodine has been observed. The population inversion was achieved by flash photolysis of trifluoromethyl iodide. A gain of e^7 was measured for a laser probe pulse at the anti-Stokes wavelength passing through the inverted iodine coincident with a laser pump pulse. This result is in good agreement with theoretical predictions.

In the presence of intense electromagnetic radiation of optical frequency ω_1 , atoms in an excited metastable state of energy $\hbar\omega_0$ can decay through enhanced two-photon emission¹ and anti-Stokes Raman scattering.² In the first process, two photons are emitted with frequencies ω_1 and $\omega_2 = \omega_0 - \omega_1$. In the second process, the incident photon is absorbed and simultaneously a photon of energy $\omega_2 = \omega_0 + \omega_1$ is emitted. If the intensity at frequency ω_2 becomes sufficiently large, these emission processes will be stimulated. Resonant stimulated anti-Stokes Raman scattering has been observed by Sorokin *et al.*³ in potassium vapor in which a population inversion between the two 4^2P excited states was produced through absorption of laser light by atoms in the $4^2S_{1/2}$ ground state. In this Letter we report the first observation of nonresonant stimulated anti-Stokes Raman scattering (ASRS) in a medium in which a population inversion was produced by an incoherent pumping source. An inversion between the $5^2P_{3/2}$ ground state and the metastable $5^2P_{1/2}$ excited state of atomic iodine was achieved by flash

photolysis of trifluoromethyl iodide (CF_3I). The ASRS was then observed by measuring the gain at the anti-Stokes wavelength experienced by a laser probe pulse as it passed through the inverted iodine coincident with a $1.06\text{-}\mu\text{m}$ laser pump pulse. Since the iodine metastable energy $\hbar\omega_0 = 7604\text{ cm}^{-1}$ was less than the incident photon energy $\hbar\omega_1 = 9391\text{ cm}^{-1}$, only the anti-Stokes Raman decay process could occur. The possible use of ASRS in iodine to produce frequency up-conversion of high-power lasers was recently suggested by Vinogradov and Yukov.⁴

The experimental arrangement used is shown in Fig. 1. The neodymium-doped yttrium aluminum garnet oscillator⁵ was electro-optically Q switched permitting reliable time synchronization between the laser pulse and the flashlamp discharge used to invert the iodine. The oscillator produced a train of pulses each of 0.75-nsec duration with a transform-limited bandwidth of 0.020 cm^{-1} . The pulse duration was as short as possible, consistent with the limit imposed by steady-state Raman scattering theory,